

Wright State University

CORE Scholar

Physics Faculty Publications

Physics

9-1-2010

Deep Traps in AlGaN/GaN Heterostructures Studied by Deep Level Transient Spectroscopy: Effect of Carbon Concentration in GaN Buffer Layers

Z-Q. Fang

B. Claflin

David C. Look

Wright State University - Main Campus, david.look@wright.edu

D. S. Green

R. Vetury

Follow this and additional works at: <https://corescholar.libraries.wright.edu/physics>



Part of the [Physics Commons](#)

Repository Citation

Fang, Z., Claflin, B., Look, D. C., Green, D. S., & Vetury, R. (2010). Deep Traps in AlGaN/GaN Heterostructures Studied by Deep Level Transient Spectroscopy: Effect of Carbon Concentration in GaN Buffer Layers. *Journal of Applied Physics*, 108 (6), 63706.
<https://corescholar.libraries.wright.edu/physics/166>

This Article is brought to you for free and open access by the Physics at CORE Scholar. It has been accepted for inclusion in Physics Faculty Publications by an authorized administrator of CORE Scholar. For more information, please contact library-corescholar@wright.edu.

Deep traps in AlGaIn/GaN heterostructures studied by deep level transient spectroscopy: Effect of carbon concentration in GaN buffer layers

Z.-Q. Fang,^{1,a)} B. Claflin,¹ D. C. Look,¹ D. S. Green,² and R. Vetury²

¹Semiconductor Research Center, Wright State University, Ohio 45435, USA and Materials and Manufacturing Directorate, Air Force Research Laboratory, Wright Patterson AFB, Ohio 45433, USA

²Defense and Power, RF Micro Devices, Inc., Charlotte, North Carolina 28269, USA

(Received 19 April 2010; accepted 1 August 2010; published online 17 September 2010)

Electrical properties, including leakage currents, threshold voltages, and deep traps, of AlGaIn/GaN heterostructure wafers with different concentrations of carbon in the GaN buffer layer, have been investigated by temperature dependent current-voltage and capacitance-voltage measurements and deep level transient spectroscopy (DLTS), using Schottky barrier diodes (SBDs). It is found that (i) SBDs fabricated on the wafers with GaN buffer layers containing a low concentration of carbon (low-[C] SBD) or a high concentration of carbon (high-[C] SBD) have similar low leakage currents even at 500 K; and (ii) the low-[C] SBD exhibits a larger (negative) threshold voltage than the high-[C] SBD. Detailed DLTS measurements on the two SBDs show that (i) different trap species are seen in the two SBDs: electron traps A_x (0.9 eV), A_1 (0.99 eV), and A_2 (1.2 eV), and a holelike trap H_1 (1.24 eV) in the low-[C] SBD; and electron traps A_1 , A_2 , and A_3 (~ 1.3 eV), and a holelike trap H_2 (> 1.3 eV) in the high-[C] SBD; (ii) for both SBDs, in the region close to GaN buffer layer, only electron traps can be detected, while in the AlGaIn/GaN interface region, significant holelike traps appear; and (iii) all of the deep traps show a strong dependence of the DLTS signal on filling pulse width, which indicates they are associated with extended defects, such as threading dislocations. However, the overall density of electron traps is lower in the low-[C] SBD than in the high-[C] SBD. The different traps observed in the two SBDs are thought to be mainly related to differences in microstructure (grain size and threading dislocation density) of GaN buffer layers grown at different pressures. © 2010 American Institute of Physics. [doi:10.1063/1.3488610]

I. INTRODUCTION

One of the major issues that limit the performance of AlGaIn/GaN heterostructure field effect transistor (HFET) devices for next generation high-power and high-frequency electronics is the presence of electronic traps in the device structure. Early studies revealed that gate lag and drain current collapse in HFET devices were related to traps in the AlGaIn surface and GaN buffer layers.¹ Many techniques, such as photoionization spectroscopy,² deep level transient spectroscopy (DLTS),³ deep level optical spectroscopy (DLOS),^{4,5} and current-DLTS on HFETs,⁶ have been used to study traps in AlGaIn/GaN structures. Carbon is a common residual impurity in unintentionally doped (UID) GaN buffer layers grown by metalorganic chemical vapor deposition (MOCVD) but the carbon concentration and resistivity in these layers can be controlled by growth pressure.⁷ To increase the breakdown voltage and decrease drain leakage current of HFET devices, growth of GaN buffer layers with optimal resistivity and carbon concentration is necessary. In this work, we use temperature dependent current-voltage (I-V) and capacitance-voltage (C-V) measurements as well as DLTS measurements at different depths, different rate windows, and different filling pulse widths to investigate the effect of carbon concentration, [C], in the GaN buffer layer on deep traps in present in AlGaIn/GaN devices.

II. EXPERIMENTAL

The AlGaIn/GaN heterostructure used in this study consisted of an AlN nucleation layer, an UID GaN buffer layer (~ 2 μm thick), and an UID AlGaIn layer (~ 22.5 nm thick), with an Al mole fraction of 25%, all grown by MOCVD on a SiC substrate. The carbon concentration in the buffer layer was primarily controlled by growth pressure. Two wafers, one grown at 500 Torr and having a low [C] in the buffer layer and one grown at 100 Torr containing a high [C], were evaluated in this study. According to Wickenden *et al.*,⁷ carbon incorporation decreases from 4×10^{17} to 5×10^{16} cm^{-3} with an increase in growth pressure from 65 to 500 Torr. Each wafer was patterned with HFETs, Schottky barrier diodes (SBDs), and van der Pauw (VDP) structures and VDP and SBD samples were cut close to the center of each wafer for Hall-effect and DLTS measurements. Temperature-dependent (20–320 K) Hall-effect measurements were performed with a Lakeshore 7507 system and show similar electrical properties for samples with low- and high-[C]: mobility $\mu = 6900$ $\text{cm}^2/\text{V s}$ and 1600 $\text{cm}^2/\text{V s}$, and sheet charge concentration $n = 1 \times 10^{13}$ cm^{-2} and 9.6×10^{12} cm^{-2} , at 20 K and 300 K, respectively. In the SBD samples, Schottky dot (125 μm in diameter), and ring-shaped Ohmic contact surrounding the dot were fabricated on the surface using Ni/Au and Ti/Al/Ni/Au metallizations, respectively. The 25 μm region between the Schottky dot and Ohmic contact was passivated with Si_3N_4 . The C-V and DLTS measurements were carried out using an Accent

^{a)}Electronic mail: zhaoqiang.fang@wright.edu.

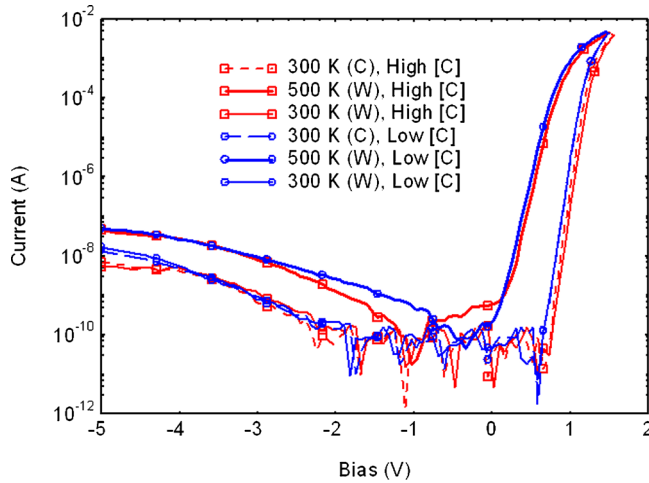


FIG. 1. (Color online) I-V characteristics, measured upon warming from 300 to 500 K and cooling to 300 K for high-[C] and low-[C] samples [symbols (W)=warming and (C)=cooling].

DL8000 spectrometer, which is operated at 1 MHz, with a test signal of 100 mV. DLTS spectra were obtained from Fourier transformation of capacitance transients, measured over a transient period, as the temperature is swept from 300 to 550 K. The I-V measurements were conducted using a current amplifier incorporated into the spectrometer. Before any measurements of temperature dependent I-V and C-V characteristics were performed, the SBD samples were warmed to 500 K and then cooled to 300 K to avoid illumination effects from a microscope light which was used during sample mounting. To determine the location of traps in the AlGaIn/GaN structure, DLTS measurements were performed at a constant bias (U_R), but with different filling pulse heights (U_p), corresponding to regions either close to the GaN buffer layer or AlGaIn/GaN interface. Different DLTS transient periods (T_W) were used to determine the activation energies of major electron and hole traps. Finally, to determine whether a measured trap is related to extended defects, DLTS measurements were performed as a function of filling pulse width (t_p). A logarithmic dependence of DLTS signal with t_p indicates that a given trap is related to extended defects (e.g., threading dislocations).³

III. RESULTS AND DISCUSSION

Figures 1 and 2 present the I-V-T and C-V-T characteristics for the two SBDs, measured at 300 and 500 K upon warming and at 300 K upon cooling. From the I-V-T curves, we see that (i) the forward currents at 300 and 500 K for both SBDs increase exponentially with bias as expected for thermionic emission; (ii) the reverse leakage currents for both SBDs are quite low even at 500 K. However, the high-[C] sample leakage is lower than that of the low-[C] sample at 300 K and is nearly constant for $U_R < -4$ V [due to complete depletion of the two-dimensional electron gas (2DEG)]; and (iii) the 300 K I-V characteristics for both SBDs show good reproducibility before and after heating to 500 K. However, as presented in Fig. 2, two differences in C-V-T characteristics are observed for these two samples. First, the 300 K C-V characteristics, measured upon warming and cooling,

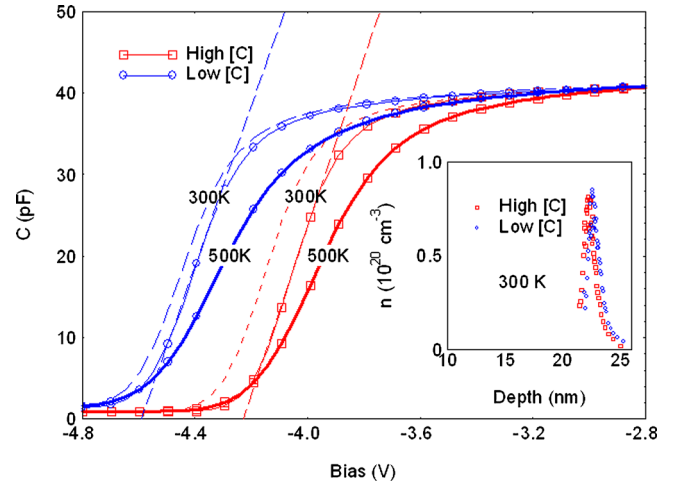


FIG. 2. (Color online) C-V characteristics, measured upon warming from 300 to 500 K and cooling to 300 K, for high-[C] and low-[C] samples (at 300 K, dashed lines=warming from 300 K and solid lines=cooling to 300 K).

show remarkable change due to an illumination effect, i.e., a shift in the 300 K threshold voltage (V_{th}) by ~ 0.05 V for the low-[C] SBD and by ~ 0.1 V for the high-[C] SBD. The illumination effect arises because deep traps can be optically filled by the illumination at 300 K and thermally emptied by warming to 500 K or higher temperatures. Second, as compared to that of the high-[C] SBD, the low-[C] SBD shows a more negative V_{th} (by ~ -0.4 V), which is likely due to lower [C] and resistivity in the GaN buffer layer, grown at higher pressure. Variation in V_{th} with GaN buffer growth pressure has been reported for devices on the AlGaIn/GaN heterostructures grown on Si substrates.¹⁶ In that study, it was found that the variation was about 0.5 V when the growth pressure changed from 200 to 760 Torr; however, at the lowest growth pressure (100 Torr), the V_{th} showed a large variation (about 2.5 V). This variation was believed to be due to the variation in sheet carrier concentration. However, in this study, we find that variation in sheet carrier concentration in the two wafers is very slight (i.e., a little higher at 300 K in the low-[C] sample), which was further confirmed by similar 2DEG densities, deduced from C-V characteristics. The shift in V_{th} might be due to a slight difference in the thickness of the AlGaIn cap. As shown in the inset of Fig. 2, the 2DEG carrier density is about the same for both SBDs but there is a slight difference in thickness of the AlGaIn cap (22.7 nm for the low-[C] SBD and 22.3 nm for the high-[C] SBD). Another possible reason for the V_{th} shift might be the difference in density of shallow traps in the two SBD samples; i.e., there could be more shallow traps in the low-[C] sample than in the high-[C] sample. According to Kordos *et al.*,⁸ the threshold voltage can be described as $V_{th} = \Phi_b - \Delta E_c - (qn_{tot}d/2\epsilon_r\epsilon_0)$, where Φ_b is the barrier height, ΔE_c is the conduction band discontinuity, d is the barrier-channel distance, and $\epsilon_r\epsilon_0$ is the dielectric constant. The total carrier density n_{tot} is a sum of the densities of shallow carriers and carrier traps, $n_{tot} = n_s + n_T$. A shift in V_{th} to a more negative value has been reported for the AlGaIn/GaN SBDs after 1 MeV electron-irradiation (EI), which is attributed to the EI-induced shallow traps.⁹

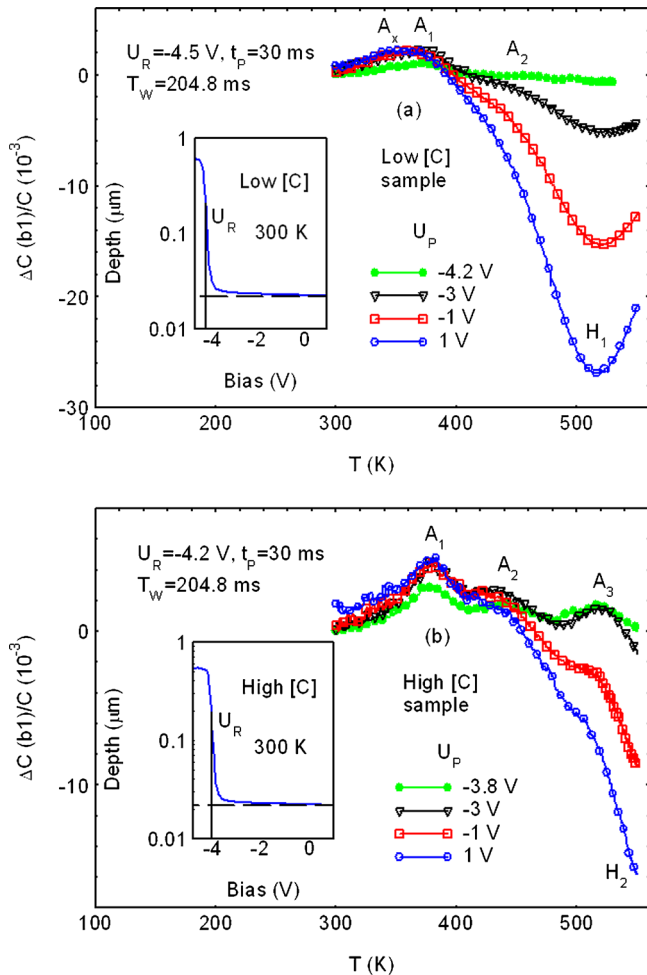


FIG. 3. (Color online) DLTS spectra as a function of filling pulse height (U_p) (a) from 1 to -4.2 V, keeping $U_R = -4.5$ V, for the low-[C] sample and (b) from 1 to -3.8 V, keeping $U = -4.2$ V, for the high-[C] sample.

Because of the different V_{th} observed in the two SBD samples, U_R was selected differently (-4.5 V for the low-[C] SBD and -4.2 V for the high-[C] SBD) to ensure that DLTS measurements are made in the pinch-off region. DLTS spectra, measured as a function of U_p , while keeping reverse bias (U_R) constant, are presented in Figs. 3(a) and 3(b) for the low-[C] and high-[C] SBDs, respectively. From the depth versus bias relationship, which is extracted from C-V data and shown in the insets of Figs. 3(a) and 3(b), the corresponding depths for the two U_R values chosen is about $0.15 \mu\text{m}$. Three U_p values were used for each SBD ($U_p = 1, -1, -3$ V) which corresponds to DLTS detection in regions close to and across the 2DEG channel (or AlGaIn/GaN interface region). The fourth values, $U_p = -4.2$ V for the low-[C] SBD and $U_p = -3.8$ V for the high-[C] SBD, corresponds to DLTS detection only in the pinch-off region close to the GaN buffer layer. From Figs. 3(a) and 3(b), we see (i) electron traps A_x , A_1 , and A_2 at $U_p = -4.2$ V in the low-[C] SBD; (ii) electron traps A_1 , A_2 , and A_3 at $U = -3.8$ V in the high-[C] SBD; and (iii) overall trap densities are higher in the high-[C] SBD than in the low-[C] SBD, but not for H traps. As U_p increases to -3 V, corresponding to detection near the 2DEG channel, we observe (i) the appearance of a negatively going holelike trap H_1 at 510 K in the low-[C]

SBD and a holelike trap H_2 at $T > 550$ K in the high-[C] SBD; and ii) an increase in traps A_x and A_1 in the low-[C] sample and A_1 and A_2 in the high-[C] sample, which is due to an increase in the detection volume. As U_p further increases from -3 to 1 V, corresponding to detection across the 2DEG channel, we observe i) a significant increase in H_1 in the low-[C] SBD and H_2 in high-[C] SBD (H_2 had not peaked before the upper temperature limit was reached); (ii) almost no change in the electron traps (A_x and A_1) in the low-[C] SBD and (A_1 and A_2) in the high-[C] SBD; and (iii) a significant decrease in the electron traps, A_2 in the low-[C] SBD and A_3 in the high-[C] SBD, which is due to the influence of increased negatively going H_1 and H_2 in the respective SBDs. The results mentioned above clearly indicate the existence of holelike traps in the 2DEG or interface region in the AlGaIn/GaN heterostructures, with different trap species (H_1 or H_2) in wafers with different [C] in the GaN buffer layer. Holelike traps have been previously reported for AlGaIn/GaN HFETs using current or conductance DLTS techniques.⁶ In Ref. 6, two holelike traps (0.29 and 0.55 eV) were attributed to surface states of the HFET, since they became small in devices passivated with Si_3N_4 . The two deep holelike traps (H_1 and H_2), found here in passivated SBDs which increase near the 2DEG channel, are believed to be traps located at AlGaIn/GaN heterointerface, rather than on the AlGaIn surface between the Schottky and Ohmic contacts. Such heterointerface states have recently attracted attention. For example, a planar Pt/AlGaIn/GaN SBD was characterized by C-V and DLTS measurements, and compared to a reference Pt/GaN:Si SBD.⁵ Two specific deep levels, at ~ 1.70 and ~ 2.08 eV below the conduction band, were reported, with the 1.70 eV level behaving as a hole trap as well as an electron trap. From the diode bias dependence of the steady-state photocapacitance, these levels were believed to stem from the 2DEG region at the AlGaIn/GaN heterointerface. Whether or not the 1.70 eV level has a connection with our holelike traps H_1 or H_2 requires further study.

To determine the activation energy of the dominant holelike trap H_1 in the low-[C] SBD and the electron trap A_1 in the high-[C] SBD, DLTS spectra were measured using values of T_W from 102.4 to 819.2 ms. As shown in Figs. 4(a) and 4(b), the DLTS peaks of these traps shift with T_W . In our digital DLTS system, the Arrhenius plot for a given trap can be obtained by using the “maximum evaluation” method. This method is based on an analysis of the peak temperature of a given trap obtained from the different Fourier components of the capacitance transient. From these Arrhenius plots, shown in the insets of Figs. 4(a) and 4(b), values of the activation energy and capture cross section were determined to be 1.24 eV and $5 \times 10^{-12} \text{ cm}^2$ for the holelike trap H_1 and 0.99 eV and $1.5 \times 10^{11} \text{ cm}^2$ for the electron trap A_1 . These values are similar to those observed for trap A_1 , previously reported by our laboratory for AlGaIn/GaN SBDs from other source.³ Activation energy of 0.9 eV for trap A_x was found in AlGaIn/GaN SBDs studied recently in our laboratory.⁹ Trap A_2 with activation energy of 1.2 eV was observed in bulklike GaN grown by hydride vapor phase epitaxy and irradiated with 0.4 MeV electrons, and in the electron-irradiated

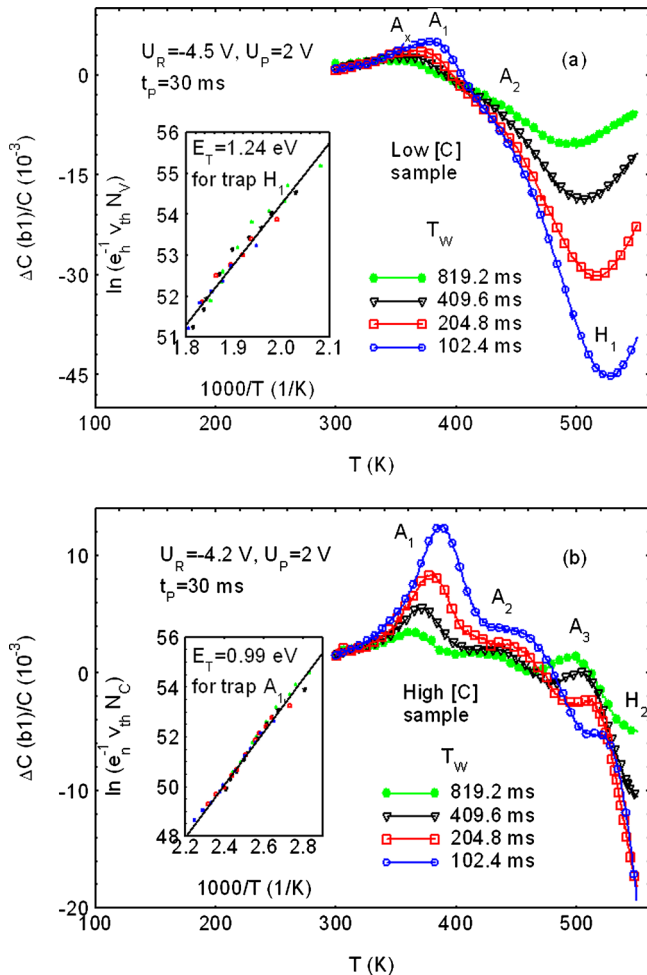


FIG. 4. (Color online) DLTS spectra as a function of transient periods (T_w) from 102.4 to 819.2 ms: (a) trap H_1 in the low $[C]$ sample and (b) trap A_1 in the high $[C]$ sample. Arrhenius plots of $\ln(e_n^{-1} v_{th} N_C)$ for H_1 and A_1 are shown in the respective insets.

AlGaIn/GaN SBDs as well.⁹ Since two traps, trap E (0.16 eV, related to the N-vacancy) and trap A_2 , were simultaneously induced by the EI, A_2 was tentatively identified as the corresponding N-interstitial. Activation energy for traps A_3 and H_2 cannot be accurately determined. Because of their peak temperatures at $T > 500$ K, they must have activation energies higher than 1.2 eV, with an estimated value of ~ 1.3 eV for the A_3 .

In AlGaIn/GaN HFETs grown by MOCVD, the role of carbon with respect to the deep traps responsible for current collapse was studied by photoionization spectroscopy.² From that study, it was found that (i) two deep traps, trap1 at 1.8 eV (which may be associated with dislocations) and trap2 at 2.85 eV [which is due to a carbon-related defect, from a comparison of its concentration with carbon concentration measured by secondary ion mass spectroscopy (SIMS)], were responsible for the current collapse; (ii) there was a substantial increase in concentration of the 2.85 eV trap at the lowest growth pressure (65 Torr), which corresponds to higher carbon incorporation and more severe current collapse; and (iii) there was a possible correlation between a deep carbon-related defect (providing a deep acceptor at 0.86 eV above the valance band) and yellow luminescence (YL)

in carbon-doped GaN. As for the carbon-related levels in UID GaN grown by MOCVD, we previously used thermally stimulated current (TSC) spectroscopy to study deep centers.¹⁰ In that case, the sample, with a thickness of ~ 1.5 μm and total dislocation density of $\sim 5 \times 10^9$ cm^{-2} , had resistivity of about 10^{10} Ω cm. At least, six TSC traps peaked at 80 $\text{K} < T < 400$ K, i.e., trap B (0.63 eV), trap B_x (0.51 eV), C_1 (0.44 eV), C (0.32 eV), D (0.23 eV), and E (0.16 eV), were observed. Interestingly, these TSC traps are all similar to DLTS traps observed in various types of n-GaN, except for B_x . In a subsequent TSC study of carbon-doped semi-insulating GaN, grown by ammonia-based molecular beam epitaxy (MBE), trap B_x (0.50 eV) was found to dominate in the high-carbon sample ($[C] = 8 \times 10^{18}$ cm^{-3}) and was tentatively assigned to C_{Ga} .¹¹ The impact of carbon on trap states in n-type GaN grown by MOCVD was also studied by both DLTS and DLOS.¹² From a comparison of the DLOS measurements on low-pressure grown codoped GaN:C:Si and atmospheric-pressure grown UID GaN, two deep levels, at 1.35 and 3.28 eV below the conduction band, were observed to have a direct relation with excess carbon incorporation. The 1.35 eV and 3.28 eV levels were believed to be due to C_1 (interstitial) and C_N (substitutional) defects, respectively. Thus, from these studies, carbon-related centers in MOCVD-grown UID GaN might include traps at 0.50 eV (B_x), 2.85 eV (trap2), 1.35 eV, 3.28 eV, and 2.2 eV (YL) centers. In this study, many deep electron and holelike traps were observed. At present, we do not know their correlation with these reported carbon-related centers. However, the trap A_3 (~ 1.3 eV) in the high $[C]$ sample could be correlated with the C_1 -related 1.35 eV level.

DLTS spectra, measured as a function of filling pulse width (t_p), for the low- $[C]$ and high- $[C]$ SBDs are presented in Figs. 5(a) and 5(b), respectively. From the two figures, we can see that both traps H_1 in the low- $[C]$ SBD and A_1 in the high- $[C]$ SBD increase with increasing t_p , exhibiting logarithmic dependence, as shown in the inset figures. This kind of dependence, as reported previously for trap A_1 in the MOCVD-grown AlGaIn/GaN heterostructure,³ is an indication of the association of both traps H_1 and A_1 in AlGaIn/GaN with extended defects, such as threading dislocations. Traps A_x and A_1 in the low- $[C]$ SBD and traps A_2 and H_2 (only half of H_2 was observed) in the high- $[C]$ SBD also appear to be associated with extended defects, since their DLTS signals show a strong t_p dependence. Actually, A_x was also reported to be related to extended defects in a previous study.⁹ Unfortunately, nothing can be judged for trap A_3 , since its peak is pulled down with increasing t_p , due to an increase in negatively going signal for the holelike trap H_2 . Thus, in the two SBDs, almost all of observed traps, which are believed to be related to either point defects (e.g., N-interstitials) or impurities (e.g., carbon), are evidently associated with extended defects, such as threading dislocations.

The capture kinetics and trapping behavior of dislocation-related electron traps have been well studied in many material systems by using DLTS. These traps often show both a logarithmic dependence of DLTS peak height on filling pulse width (t_p), and broadened asymmetrical peaks

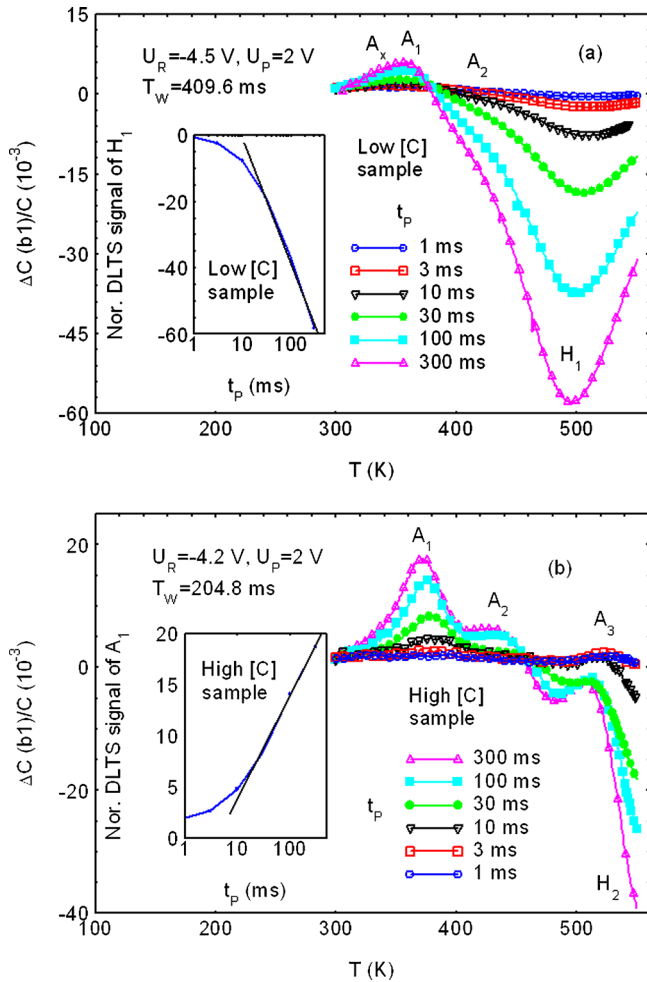


FIG. 5. (Color online) DLTS spectra as a function of filling pulse width (t_p) from 1 to 300 ms. Logarithmic dependence of normalized DLTS signal with t_p for (a) trap H_1 in the low-[C] sample and (b) trap A_1 in the high-[C] sample are shown in the respective insets.

(when the rate window is kept unchanged). A model of the time-dependent capture barrier associated with extended line defects, i.e., with the capture barrier height proportional to the number of electrons already captured, has been proposed to explain the anomalous electron capture behavior.¹³ Furthermore, as pointed out by Hierro *et al.*,¹⁴ such a capture kinetics for trap E(0.91) with activation energy of 0.91 eV in MBE-grown n-GaN [which is close to our A_x (Ref. 9)] can be explained as arising from either point defects arranged along a threading dislocation or from the threading dislocation core itself. Since point defects will generate a localized state in the bandgap whereas threading dislocation cores will create a band of states, the trap occupancy will differ. In the former case, the DLTS peak temperature would be independent of t_p , whereas in the latter case, it shifts to higher temperatures with decreasing t_p , which was observed for their trap E(0.91) and our traps H_1 and A_1 [see Figs. 5(a) and 5(b)]. Capture kinetics for a trap associated with extended defects also leads to significant change in its DLTS peak height with changing T_W (i.e., rate window) or peak temperature (when t_p is kept unchanged), as observed in Figs. 4(a) and 4(b). The reason for this change is usually not due to the temperature dependence of the capture cross section

but rather due to the relative change in the ratio t_p/T_W , as set by the DLTS measurement conditions.¹³ For major traps (such as traps A_1 , A, B, C, and D) in freestanding GaN, with low dislocation density ($5 \times 10^6 \text{ cm}^{-2}$), almost no change in the DLTS peak height is observed with change in either filling pulse width or rate window, which indicates that these traps are not associated with extended defects, but related to isolated point defects, which are not arranged along dislocations.¹³

IV. SUMMARY AND CONCLUSIONS

Now, we can summarize the differences and similarities of traps in AlGaIn/GaN heterostructures, for GaN buffer layers containing different concentrations of carbon. In the low-[C] sample, the major electron traps are A_x , A_1 , and A_2 , and a holelike trap H_1 is observed at ~ 510 K. In the high-[C] sample, the major electron traps are A_1 , A_2 , and A_3 , and a holelike trap H_2 is found at $T > 550$ K. Electron traps show lower density in the low-[C] sample than in the high-[C] sample. However, for both samples, only electron traps can be observed in the detection region close to the GaN buffer layer, and the holelike traps can be detected only near the 2DEG or interface region of AlGaIn/GaN. All traps, both electron and holelike, exhibit a strong dependence on filling pulse width, indicating their association with extended defects. These results are consistent with an early study on the relationship of GaN resistivity to film microstructure and impurity compensation by Wickenden *et al.*⁷ It was concluded from that study that (i) with increasing growth pressure, the GaN films exhibit increasing grain size, decreasing density of threading edge dislocations, decreasing carbon and oxygen concentrations, and decreasing resistivity, and (ii) threading edge dislocations play a major role in the compensation mechanism of GaN, with carbon impurity segregation at or near the threading dislocations providing compensating acceptor states. In this study, we observe that with increasing growth pressure of GaN buffer layers, AlGaIn/GaN heterostructures exhibit a variety of electron traps in the GaN buffer layer, holelike traps near the AlGaIn/GaN interface, decreasing dislocation-related electron traps, and decreasing carbon concentration. Further study on the impact of these traps on HFET device performance, such as current collapse and reliability, is needed. A good correlation between current collapse of AlGaIn/GaN HFET wafers grown on silicon substrates and YL (~ 2.2 eV) intensity has been found by scientists at Toshiba Corp.¹⁵ It is necessary to further study correlation between the deep holelike traps (H_1 and H_2) and the YL. In writing this paper, a study about effect of GaN buffer layer growth pressure on the device characteristics of AlGaIn/GaN HEMTs on Si was published.¹⁶ In that study, it was found that the formation of highly resistive buffer with [C] as high as $3.8 \times 10^{17} \text{ cm}^{-3}$ (for GaN grown at 200 Torr pressure) leads to reduced buffer leakage over one order of magnitude and enhanced breakdown voltage of 425 V for a HEMT with gate-drain spacing of 4 μm . However, unlike samples grown at atmospheric

pressure, the presence of unintentional C in the semi-insulating GaN degraded the channel conduction and resulted in severe current collapse.

ACKNOWLEDGMENTS

We would like to thank Dr. Donald Dorsey for encouragement and support, and Tim Cooper for Hall-effect measurements. This work was performed by the AFRL-lead National High Reliability Electronics Virtual Center (HiREV). The work of Z.-Q.F., B.C., and D.C.L. was directly supported by AFRL's Materials & Manufacturing Directorate under Contract No. FA8650-06-D-5401.

- ¹S. C. Binari, K. Ikossi, J. A. Roussos, W. Kruppa, D. Park, H. B. Dietrich, D. D. Koleske, A. E. Wickenden, and R. L. Henry, *IEEE Trans. Electron Devices* **48**, 465 (2001).
²P. B. Klein, S. C. Binari, K. Ikossi, A. E. Wickenden, D. D. Koleske, and R. L. Henry, *Appl. Phys. Lett.* **79**, 3527 (2001).
³Z.-Q. Fang, D. C. Look, D. H. Kim, and I. Adesida, *Appl. Phys. Lett.* **87**, 182115 (2005).
⁴A. Armstrong, A. Chakraborty, J. S. Speck, S. P. DenBaars, U. K. Mishra, and S. A. Ringel, *Appl. Phys. Lett.* **89**, 262116 (2006).
⁵Y. Nakano, Y. Irokawa, and M. Takeguchi, *Appl. Phys. Express* **1**, 091101

(2008).

- ⁶T. Mizutani, T. Okino, K. Kawada, Y. Ohno, S. Kishimoto, and K. Maezawa, *Phys. Status Solidi A* **200**, 195 (2003).
⁷A. E. Wickenden, D. D. Koleske, R. L. Henry, M. E. Twigg, and M. Fatemi, *J. Cryst. Growth* **260**, 54 (2004).
⁸P. Kordoš, D. Donoval, M. Florovič, J. Kováč, and D. Gregušová, *Appl. Phys. Lett.* **92**, 152113 (2008).
⁹Z.-Q. Fang, G. C. Farlow, B. Claflin, D. C. Look, and D. S. Green, *J. Appl. Phys.* **105**, 123704 (2009).
¹⁰Z.-Q. Fang, B. Claflin, D. C. Look, T. H. Myers, D. D. Koleske, A. E. Wickenden, and R. L. Henry, *GaN and Related Alloys-2002*, MRS Symposia Proceedings No. 743 (Materials Research Society, Pittsburgh, 2005), p. 749.
¹¹Z.-Q. Fang, D. C. Look, B. Claflin, S. Haffouz, H. Tang, and J. Webb, *Phys. Status Solidi C* **2**, 2757 (2005).
¹²A. Armstrong, A. R. Arehart, B. Moran, S. P. DenBaars, U. Mishra, J. S. Speck, and S. A. Rengel, *Appl. Phys. Lett.* **84**, 374 (2004).
¹³Z.-Q. Fang, D. C. Look, and L. Polenta, *J. Phys.: Condens. Matter* **14**, 13061 (2002).
¹⁴A. Hierro, A. R. Arehart, B. Heying, M. Hansen, J. S. Speck, U. K. Mishra, S. P. DenBaars, and S. A. Ringel, *Phys. Status Solidi B* **228**, 309 (2001).
¹⁵H. Fujimoto, W. Saito, A. Yoshioka, T. Nitta, Y. Kakiuchi, and Y. Saito, *CS MANTECH Dig.* 5.2 (2008).
¹⁶J. Selvaraj, S. L. Selvaraj, and T. Egawa, *Jpn. J. Appl. Phys., Part 2* **48**, 121002 (2009).